Pyrene-sensitized electron transport across vesicle bilayers: dependence of transport efficiency on pyrene substituents†

Tadashi Mizushima, Asako Yoshida, Akitomo Harada, Yu Yoneda, Tomiaki Minatani and Shigeru Murata*

Received 4th July 2006, Accepted 6th October 2006
First published as an Advance Article on the web 24th October 2006
DOI: 10.1039/b609507k

Endoergic electron transport across vesicle bilayers from ascorbate (Asc^-) in the inner waterpool to methylviologen (MV^{2+}) in the outer aqueous solution was driven by the irradiation of pyrene derivatives embedded in the vesicle bilayers. The initial rate of MV^{2+} reduction is dependent on the substituent group of the pyrenyl ring; a hydrophilic functional group linked with the pyrenyl ring by a short methylene chain acts as a sensitizer for the electron transport. Mechanistic studies using (1-pyrenyl)alkanoic acids (**1a–c**) as sensitizers suggest that the electron transport is mainly initiated by the reductive quenching of the singlet excited state of the pyrene by Asc^- and proceeds by a mechanism involving electron exchange between the pyrenes located at the inner and outer interface across the vesicle bilayer. We designed and synthesized novel unsymmetrically substituted pyrenes having both a hydrophilic group linked by a short methylene chain and a hydrophobic long alkyl group (**5a–c**), which acted as excellent sensitizers for the electron transport across vesicle bilayers.

Introduction

Natural photosynthesis in green plants, algae, or bacteria is a highly efficient energy conversion system, in which solar energy is converted into chemical potential and stored in carbohydrates.[1] From a photochemical point of view, photosynthesis can be described as a photoinduced redox reaction, where electrons are transferred from water to the oxidized form of nicotinamide adenine dinucleotide phosphate ($NADP^+$) to produce NADPH required for reduction of CO_2 to carbohydrates. Attempts to mimic natural photosynthetic systems may lead to the construction of simpler models to understand natural systems, but also to the production of artificial systems to convert light energy into chemical potential with high efficiency.[2]

The phospholipid bilayer membrane plays an essential role in natural photosynthesis. The photosynthetic membrane, which is called the thylakoid membrane, not only supports lipid–protein complexes containing pigments that participate in light absorption and charge separation, but acts as a barrier to inhibit the undesirable recombination reaction between photogenerated oxidizing and reducing species. Researches on the photoinduced redox reaction mimicking natural photosynthetic systems have progressed using vesicles as a model of the thylakoid membrane. Vesicles are spherical, multimolecular aggregates formed by self-organization of natural or synthetic amphiphiles, in which a hydrophobic lipid bilayer separates an inner waterpool from the bulk aqueous phase.[3] In 1978, Calvin and his coworkers clearly demonstrated that the reduction of methylviologen (*N*,*N*′-dimethyl-4,4′-bipyridinium, MV^{2+}) dissolved in the outer aqueous phase of a phospholipid vesicle solution could be sensitized by the tris(bipyridine)ruthenium derivative that existed in the hydrophobic lipid bilayer when EDTA was dissolved in the inner waterpool of the vesicle.[4] Since then, various systems of photo-induced electron transport across vesicle bilayers for exploring the mechanism and efficiency have been presented, and their applications such as the photochemical decomposition of water into hydrogen and oxygen have been investigated.[5] Very recently, Hurst and his colleagues reported on a vesicle system in which electron transport from EDTA in the outer aqueous phase to Co^{3+} in the inner waterpool proceeded by employing the water-soluble zinc tetraphenylporphyrin and anthraquinone derivatives as a sensitizer and a transmembrane electron carrier, respectively.[6] Although the studies presented so far reveal the usefulness of vesicles for mimicking natural photosynthetic systems, further studies are required to reach the final goal, *i.e.*, the construction of artificial systems capable of converting light energy into chemical potential with high efficiency.

In order for light–chemical energy conversion to mimic natural photosynthetic systems, systems of photoinduced electron transport across vesicle bilayers should satisfy the following four criteria. First, the total redox reaction should be endoergic with a positive free-energy change, ΔG. Second, both oxidative and reductive reactions should be reversible. When sacrificial electron donors such as EDTA and triethanolamine, which decompose irreversibly, are used to suppress the recombination of photo-generated charges, a reducing species can be generated even in homogeneous solutions converting light energy in total. Third, an electron transport is induced by the excitation of the sensitizer embedded in the vesicle bilayers, and proceeds from the donor incorporated in the inner waterpool to the acceptor dissolved in the outer aqueous solution. This vectorial electron transport makes it possible to employ photo-generated electrons for useful

Department of Basic Science, Graduate School of Arts and Sciences, The University of Tokyo, Meguro-ku, Tokyo 153-8902, Japan. E-mail: cmura@mail.ecc.u-tokyo.ac.jp; Fax: +81 3 5454 6998

† Electronic supplementary information (ESI) available: Preparation of sensitizers **1b**, **2b**, **3b**, **4a**, **4b**, and **5a–c**; derivation of eqn 3; particle size distribution; $MV^{+\bullet}$ accumulation data; fluorescence spectra of **1a** in various solvents; dependence of $MV^{+\bullet}$ accumulation rate on light intensity; fluorescence spectra of **5b** and **5c** in the vesicle solution. See DOI: 10.1039/b609507k

reductive processes such as hydrogen production from water and the conversion of CO_2 into fuel. Finally, electron transport is driven by visible light to achieve high efficiency of light–chemical energy conversion. Among the number of systems of photoinduced electron transport across vesicle bilayers reported so far, there are very few systems that meet these criteria.[7,8]

In the course of our studies on pyrene-sensitized photoreactions,[9] we found that pyrene derivatives embedded into the bilayers of phosphatidylcholine (PC) vesicles photochemically induce transport of electrons from ascorbate (Asc^-) entrapped into the inner waterpool to MV^{2+} dissolved in the outer aqueous solution without any additional components acting as electron carriers.[10] The free-energy change for the total redox reaction of our electron transfer system is estimated to be +12.7 kcal mol^{-1}.[11,12] Thus, although the pyrenes employed in our experiments unfortunately do not absorb visible light (>400 nm), this system satisfies the other three criteria mentioned above. This is the first report on employing pyrenes as sensitizers of electron transport across vesicle bilayers, although charge separation sensitized by pyrene-substituted lipid molecules incorporated in lipid bilayers has already been reported.[13]

Pyrenes have several advantages as sensitizers for electron transport across vesicle bilayers. First, a wide variety of their derivatives can easily be prepared, which enables us to study the electron transport mechanism systematically and to control the transport efficiency. Second, pyrenes have a long lifetime of their singlet excited state (>100 ns), which is favorable for electron transfer from or to quenchers. Third, since pyrenes have been widely employed as the fluorescent probe to characterize the polarity or fluidity of vesicle bilayers,[14] information on the behaviors of pyrenes in vesicle bilayers is available. Finally, photophysical properties of pyrenes are well-known,[9b,15] so that the short-lived reactive species that would intervene in the electron transport can be detected and identified easily. In this paper, we report the remarkable dependence of the ability to sensitize electron transport on the substituent group introduced into the pyrene nucleus, and design and synthesize new pyrene derivatives which act as excellent sensitizers for an electron transport across vesicle bilayers.

Results and discussion

Accumulation of methylviologen radical cation ($MV^{+\bullet}$) by the irradiation of vesicle solutions

Vesicle solutions used for photoinduced electron transport experiments were prepared as follows; a suspension of (1-pyrenyl)acetic acid (**1a**) and PC from egg yolks in 1.0 M tris(hydroxymethyl)-aminomethane–HCl (Tris–HCl) buffer (pH 7.5) containing AscNa (1.0 M) was sonicated under Ar for 60 min at 45 °C. The suspension was developed by chromatography on a Sephadex G-50 column with a buffer solution containing NaCl (1.0 M) to remove the electron donor and the sensitizer outside the vesicles, and then $MVCl_2 \cdot 3H_2O$ was added to give a vesicle solution with MV^{2+} (10 mM) in an outer aqueous phase. By measurement of the particle size distribution of the solution using a dynamic light-scattering method, the formation of particles with a diameter of 40–100 nm was confirmed indicating that the majority of the vesicles had a unilamellar structure (Fig. S1†). Incorporation of **1a** into the vesicle solution was monitored by its UV absorption with a maximum at around 342 nm. As shown in the following section, although the molar ratio of the pyrene derivative to PC was identical (4.3 mol%) in the vesicle preparation, the concentration of the pyrene derivative incorporated in the vesicle solution, C_s, was dependent on the substituent group on the pyrenyl ring.

On the irradiation of the vesicle solution containing **1a** (C_s = 5.4 μM) as a sensitizer with a 500-W xenon arc lamp through a band pass filter (360 ± 20 nm),[16] the accumulation of $MV^{+\bullet}$, which was readily identified by its characteristic absorption with maxima at 396 and 604 nm, was observed (Fig. 1). An increase in the concentration of $MV^{+\bullet}$, $[MV^{+\bullet}]$, with irradiation time, t, obeyed good first-order kinetics,

$$[MV^{+\bullet}] = A_m[1 - \exp(-k_{obs}t)] \quad (1)$$

from which the initial rate of $MV^{+\bullet}$ formation, v_i, was evaluated as $A_m k_{obs}$. Neither change in the particle size distribution nor significant consumption of the sensitizer was observed after the irradiation.

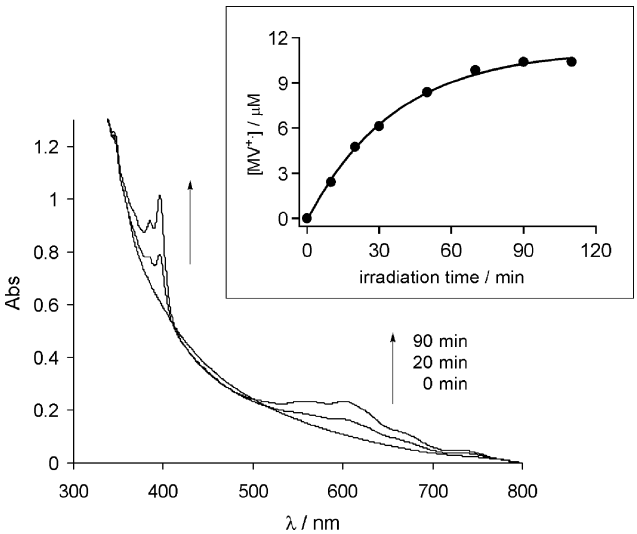

Fig. 1 Accumulation of $MV^{+\bullet}$ by the irradiation of a solution of vesicles containing **1a** and Asc^-. The inset figure shows the change in the concentration of $MV^{+\bullet}$ *vs.* irradiation time, together with the curve fitted to the experimental data according to eqn (1).

Evidence for electron transport across vesicle bilayers

The following three experimental results indicate that the generation of $MV^{+\bullet}$ by irradiation of the vesicle solution is derived from electron transport from Asc^- entrapped in the inner waterpool to MV^{2+} dissolved in the outer aqueous phase across vesicle bilayers, which is sensitized by **1a** incorporated in the hydrophobic vesicle walls.

(1) When a sufficient amount of surfactant (Triton X-100) to dissolve the vesicles was added to the vesicle solution, the initial rate of $MV^{+\bullet}$ formation, v_i, was considerably reduced to less than 5% (Fig. S2†). This observation indicates that the hydrophobic vesicle walls play an essential role in the accumulation of $MV^{+\bullet}$, suppressing the recombination reaction between photo-generated $MV^{+\bullet}$ and the oxidized form of Asc^-.

(2) When the vesicle solution was prepared according to an identical method to those described above, except for using a buffer solution containing NaCl (1.0 M) instead of AscNa, the amount of accumulated $MV^{+\bullet}$ was considerably reduced.[17,18] Furthermore, measurement of the AscNa concentration of the irradiated vesicle solution revealed that Asc^- was consumed with the accumulation of $MV^{+\bullet}$, although the amount of consumed donors was much larger than that of photo-generated $MV^{+\bullet}$ (Fig. S4†). These results imply that Asc^- entrapped into the inner waterpool acts as a principal electron donor to reduce MV^{2+}.

(3) The results of the control experiment confirmed that the pyrene **1a** was essential for the accumulation of $MV^{+\bullet}$. The location of **1a** in the vesicle solution was determined as follows. The vibronic fine structure of pyrene fluorescence is very sensitive to the solvent environment.[19] In polar solvents, the intensity of the 0–0 band (band 1) is enhanced whereas there is little effect on that of the 0–2 band (band 3), thus the ratio of the fluorescence intensities, I_1/I_3, can be used as an indication of solvent polarity, which is called the *Py* scale and is reported to have excellent correlations with other scales of solvent polarity such as Y and E_T values.[19] We applied this method to understanding the environment of **1a** in the vesicle solution. The fluorescence spectra of **1a** were measured in 10 solvents having different solvent polarity (Fig. S5†). As shown in Fig. 2, the ratio of intensities of fluorescence vibronic bands, I_1/I_3, was dependent on solvent polarity; large values of I_1/I_3 were observed in polar solvents. The I_1/I_3 value of **1a** in the vesicle solution prepared by the method described above was 1.85, which is intermediate between the values of protic and aprotic polar solvents. Based on this observation, we conclude that the sensitizer **1a** is not located in bulk aqueous solutions, but in the membrane interior close to the bilayer–water interface. Taking into account the dissociation of the carboxyl group into the hydrophilic carboxylate ion under the pH condition employed in our experiments, it appears that the carboxylate group is anchored at the bilayer–water interface with the pyrene moiety extending into the membrane interior. This assumption is consistent with the conclusion obtained by Galla and his coworkers who determined the location of the pyrene moiety of ω-(1-pyrenyl)alkanoic acids in lipid bilayers by the use of paramagnetic quenching of their fluorescence.[20]

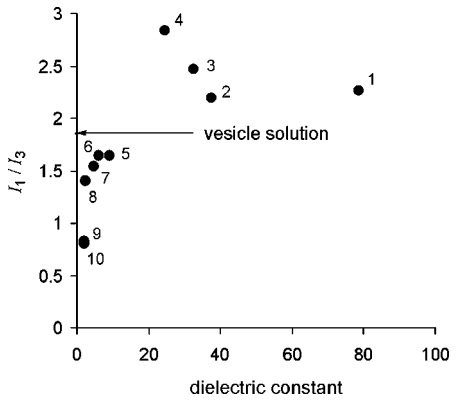

Fig. 2 Plots of the ratio of vibronic band intensities of fluorescence of **1a** *vs.* the dielectric constant of the solvent: 1, water; 2, acetonitrile; 3, methanol; 4, ethanol; 5, dichloromethane; 6, ethyl acetate; 7, chloroform; 8, benzene; 9, cyclohexane; 10, octane. The arrow shows the value in the vesicle solution (1.85).

Dependence of sensitizer ability on the substituent group of the pyrene nucleus

To optimize the structure of pyrenes employed as sensitizers for electron transport across vesicle bilayers, the dependence of sensitizer ability, which is evaluated with the initial rate of $MV^{+\bullet}$ formation, v_i, as well as the maximal concentration of photo-generated $MV^{+\bullet}$, C_{max}, on the substituent group at the 1-position of the pyrene nucleus was investigated. It was first found that the formation of $MV^{+\bullet}$ was not observed when unsubstituted pyrene was employed as a sensitizer, thus we examined the pyrenes having the structure of $Py(CH_2)_nX$ (Py = 1-pyrenyl, X = H or substituent group) systematically. The vesicle solution was prepared in an identical manner to that described in the previous section, except for using these pyrenes instead of **1a**, and irradiated. The v_i and C_{max} determined by the electron transport experiments, as well as the concentration of the pyrenes incorporated in the vesicle solution, C_s, are summarized in Table 1, showing that the sensitizer ability is dependent on the substituent group of the pyrene

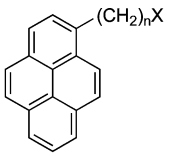

1; X = CO_2H, **a**; n = 1, **b**; n = 2, **c**; n = 3
2; X = NH_2, **a**; n = 1, **b**; n = 2
3; X = OH, **a**; n = 1, **b**; n = 2
4; X = H, **a**; n = 2, **b**; n = 8

Table 1 Electron transport across vesicle bilayers sensitized by the pyrene derivatives $Py(CH_2)_nX$

$-(CH_2)_nX$		$v_i/10^{-7}$ M min^{-1}	$C_{max}/\mu M$	$C_s/\mu M$	I(rel)[a]	Φ_t(rel)[b]
$-CH_2CO_2H$	(**1a**)	18.0	17.4	5.4	1.0	14.7
$-(CH_2)_2CO_2H$	(**1b**)	9.1	10.9	5.7	1.1	7.0
$-(CH_2)_3CO_2H$	(**1c**)	2.5	3.0	30	3.9	0.51
$-CH_2NH_2$	(**2a**)	53.5	30.8	35	4.4	10.0
$-(CH_2)_2NH_2$	(**2b**)	5.9	5.0	72	6.8	0.71
$-CH_2OH$	(**3a**)	44.9	16.5	66	6.4	5.7
$-(CH_2)_2OH$	(**3b**)	16.2	9.6	70	6.7	2.0
$-CH_2CH_3$	(**4a**)	<0.1	<0.1	68	6.6	<0.01
$-(CH_2)_7CH_3$	(**4b**)	<0.1	<0.1	71	6.7	<0.01

[a] Relative value of the number of photons absorbed by the sensitizer under our irradiation conditions estimated by the integration of $I_f(\lambda)(1-10^{-\varepsilon(\lambda)Csl})$ (I(rel) = 1.0 for **1a**), see text. [b] Relative value of a total quantum yield for $MV^{+\bullet}$ formation (Φ_t = 10.0 for **2a**).[21]

nucleus. The results clearly indicate the following two facts. First, a hydrophilic functional group is essential for pyrene derivatives to act as sensitizers for electron transport across vesicle bilayers. Second, the effectiveness of the hydrophilic group decreases significantly as the length of the methylene chain connecting the hydrophilic group with the pyrene nucleus is increased.

As discussed in detail in the following section, the initial rate of $MV^{+\bullet}$ formation, v_i, is governed by the product of the number of photons absorbed by the sensitizer in unit time, I, and a total quantum yield for $MV^{+\bullet}$ formation, Φ_t. The absorption spectra in the region of >300 nm of the pyrene derivative $Py(CH_2)_nX$ employed as the sensitizers are practically identical exhibiting an intense transition with a maximum at 342 nm. Since the light from a xenon arc lamp through a band-path filter (360 ± 20 nm) was employed in the irradiation, the relative value of I for each sensitizer is estimated by the integration of $I_f(\lambda)(1 - 10^{-\varepsilon(\lambda)Csl})$, where $I_f(\lambda)$ shows the wavelength dependence of incident light evaluated by the spectrum of the light transmitted by the filter employed in the electron transport experiment (360 ± 20 nm), $\varepsilon(\lambda)$ stands for the absorption spectrum of each sensitizer, and l represents the length of the cell used in the irradiation experiment. Thus, the relative quantum yields for $MV^{+\bullet}$ formation, Φ_t(rel), can be estimated by v_i/I, which are presented in Table 1.[21] As shown in the table, an increase in the hydrophobicity by the extension of the methylene chain linking the hydrophilic functional group with a pyrene nucleus results in an increase in C_s which is favorable for the rapid formation of $MV^{+\bullet}$, while it causes a considerable decrease in Φ_t which leads to a total decrease in v_i.

The dependence of the sensitizer ability on the substituent is interpreted in terms of the position of the pyrene moiety of the sensitizer relative to the bilayer–water interface. As mentioned in the previous section, the sensitizers having a hydrophilic functional group connected to a pyrene moiety by a short methylene chain are anchored at the bilayer–water interface, facilitating electron transfer processes which occur at the interface. On the other hand, the hydrophobic sensitizers are incorporated into the interior of the vesicle membrane, the position of which is unfavorable for the interaction with the electron donor and acceptor dissolved in aqueous phases. An analogous interpretation was offered in the effect of the 1-methylpyridinium moiety in the electron transport across vesicle bilayers sensitized by synthetic magnesium porphyrins.[7] On the basis of the detailed data of the reactions sensitized by (1-pyrenyl)acetic acid (**1a**) and 4-(1-pyrenyl)butyric acid (**1c**), the effect of the methylene chain length on the electron transport efficiency is further discussed in the following section.

Mechanistic studies of electron transport across vesicle bilayers sensitized by (1-pyrenyl)alkanoic acids

The data described in the previous sections indicate that the photoreduction of MV^{2+} dissolved in the outer aqueous phase of the vesicle solution is derived from the electron transport across vesicle bilayers sensitized by the pyrene derivative embedded in the vesicle membrane, in which Asc^- entrapped in the inner waterpool acts as an electron donor. Moreover, it is indicated that a total quantum yield for the electron transport, Φ_t, is dependent on the hydrophobicity of the sensitizers. In this section, we report the results of studies to elucidate the factors governing Φ_t, and propose a plausible mechanism of the electron transport across vesicle bilayers.

(1) Dependence of the initial rate of $MV^{+\bullet}$ accumulation on light intensity. First, the dependence of the initial rate of $MV^{+\bullet}$ accumulation, v_i, on the incident light intensity was examined to reveal the number of photons required to produce one molecule of $MV^{+\bullet}$. Four vesicle solutions with the same concentration of 3-(1-pyrenyl)propionic acid (**1b**) were prepared, and irradiated with light of 366 nm from an extra-high pressure mercury lamp, the intensity of which was regulated by using four kinds of neutral density filters. The initial accumulation rate, v_i, decreased with decreasing light intensity (Fig. S6†). The plot of v_i against light intensity gave a perfect straight line. A linear relationship between v_i and light intensity indicates that the photoinduced electron transport from Asc^- to MV^{2+} across vesicle bilayers requires only one photon, and excludes the possibility of electron transfer between the pyrene radical anion photogenerated in the inner bilayer–water interface and the radical cation photogenerated in the outer bilayer–water interface. Moreover, the mechanism involving a two-photon absorption ionization of pyrenes to produce a solvated electron[13a,22] is also ruled out for the formation of $MV^{+\bullet}$.

(2) Quenching of sensitizer fluorescence by MV^{2+} and Asc^-. To gain information about the initial processes of the electron transport across vesicle bilayers, quenching of the fluorescence of the pyrene sensitizers **1a–c** embedded in the vesicle bilayers by MV^{2+} and Asc^- was examined. The fluorescence intensity of **1a–c** in the vesicle solution prepared in the same manner as that described in the previous section, except that NaCl (1.0 M) was entrapped in the inner waterpool instead of AscNa, decreased by the addition of $MVCl_2$ or AscNa to the outer aqueous solution, and Stern–Volmer constants, K_{SV}, for the fluorescence quenching were obtained. The results are summarized in Table 2

Table 2 Kinetic parameters for the quenching of **1a–c** by MV^{2+} and Asc^- in PC vesicle solution and aqueous homogeneous solution

			MV^{2+}		Asc^-	
Sensitizer	System[a]	τ_s[b]/ns	K_{SV}/M^{-1}	$k_q/10^7\ M^{-1}\ s^{-1}$	K_{SV}/M^{-1}	$k_q/10^7\ M^{-1}\ s^{-1}$
1a	PC	92 (137)	54.7	59.4	3.13	3.40
	AQ	134 (146)	1250	933	251	187
1b	PC	106 (153)	65.6	61.9	4.37	4.12
	AQ	125 (141)	884	707	188	150
1c	PC	148 (199)	51.9	35.1	11.6	7.83
	AQ	122 (136)	430	355	174	144

[a] PC; in vesicle solutions where the sensitizer was incorporated in the vesicle bilayers. AQ; in aqueous homogeneous solution (1.0 M Tris–HCl buffer, pH 7.5). [b] Lifetime of the singlet excited state of the sensitizer measured under air. Lifetime under N_2 is shown in parentheses.

together with the lifetimes of the singlet excited state of the sensitizers, τ_s, determined by the use of time-resolved fluorescence spectroscopy and rate constants for the fluorescence quenching, $k_q = K_{SV}/\tau_s$. Moreover, for the sake of comparison, quenching of the fluorescence of **1a–c** by MV^{2+} and Asc^- in an aqueous solution (1.0 M Tris–HCl buffer) was examined, the data on which are presented in the table.

As shown in the table, the quenching of the pyrene fluorescence occurs more effectively by MV^{2+} than Asc^- both in the vesicle solutions and in the fluid solutions, and the k_q's in the vesicle solutions are decreased more than one order of magnitude over the corresponding k_q's in the aqueous solutions. An analogous large decrease in quenching efficiency in vesicle solutions compared with homogeneous solutions was reported by Barenholz and his coworkers in the fluorescence quenching by iodide ions of (1-pyrenyl)alkanoic acids embedded in PC vesicles.[14a] The free-energy changes for the oxidative and reductive quenching of singlet excited pyrene with MV^{2+} and Asc^- are calculated by the Rehm–Weller equation[23] to be −39 and −26 kcal mol^{-1}, respectively.[11,24] These large exothermicities suggest that both quenching processes proceed by an electron transfer mechanism. It should be noted that although MV^{2+} quenches the singlet excited state of **1a–c** more effectively than Asc^-, the efficiency of quenching with Asc^-, Φ_D, which is depicted by $k_q[Asc^-]/(\tau_s^{-1} + k_q[Asc^-])$, is much greater than that with MV^{2+}, Φ_M, owing to a high concentration of Asc^- entrapped into the inner waterpool; $\Phi_D = 0.82$, $\Phi_M = 0.45$ for **1a**. Thus, it is revealed that the reductive quenching of the singlet excited state of the sensitizer by Asc^- to produce a radical pair of the sensitizer radical anion and $Asc^{\bullet}$ plays an important role in the initiation of the electron transport across vesicle bilayers.

(3) Plausible mechanism of electron transport across vesicle bilayers. Assuming that the electron transport across vesicle bilayers is initiated by the reductive quenching of the singlet excited state of the pyrene sensitizer by Asc^- entrapped in the inner waterpool, we propose a mechanism for the formation of $MV^{+\bullet}$ as illustrated in Scheme 1. In the scheme, S_i and S_o stand for the sensitizers located in the vesicle bilayer close to the inner waterpool and the outer aqueous phase, respectively.

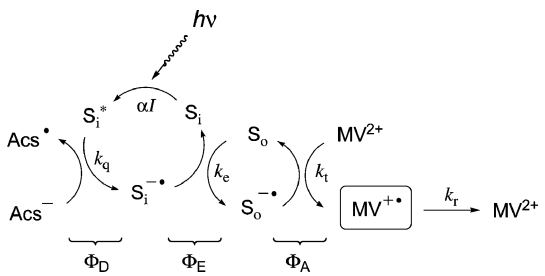

Scheme 1 Proposed mechanism for the formation of $MV^{+\bullet}$ initiated by the quenching of the singlet excited state of the pyrene sensitizer (S_i) by Asc^- entrapped in the inner waterpool.

According to the scheme, the change in the concentration of $MV^{+\bullet}$ produced by the reduction of MV^{2+} in the outer aqueous phase is described by eqn (2).

$$d[MV^{+\bullet}]/dt = k_t[S_o^{-\bullet}][MV^{2+}] - k_r[MV^{+\bullet}] \quad (2)$$

In the equation, k_t is a bimolecular rate constant for an electron transfer from $S_o^{-\bullet}$ (the radical anion of S_o) to MV^{2+}. The intermediate $S_o^{-\bullet}$ is produced by an electron transfer from $S_i^{-\bullet}$, which is generated by the reductive quenching of the excited state of S_i by Asc^- entrapped in the inner waterpool (Scheme 1). Moreover, $MV^{+\bullet}$ is lost by the reaction with an electron-accepting species,[25] such as contaminating O_2 and the oxidized form of Asc^- escaping from the inner waterpool, the pseudo-first-order rate constant for which is depicted by k_r. Applying a steady-state approximation to the reactive intermediates S_i^*, $S_i^{-\bullet}$, and $S_o^{-\bullet}$, eqn (2) is solved to give eqn (3) for $[MV^{+\bullet}]$ at a definite irradiation time, t.

$$[MV^{+\bullet}] = (aI\Phi_D\Phi_E\Phi_A/k_r)[1 - \exp(-k_r t)] \quad (3)$$

In this equation, I and Φ_D are the number of photons absorbed by the sensitizer in unit time and the quenching efficiency of the singlet excited state of the sensitizer by Asc^-, respectively, as defined in the previous section, and a is the proportion of sensitizers located at the interface of the vesicle bilayer and the inner waterpool. Furthermore, Φ_E, which is equal to $k_e[S_o]/(\tau_i^{-1} + k_e[S_o])$, shows the efficiency for $S_i^{-\bullet}$ in the transfer of an electron to S_o, where τ_i and k_e are the lifetime of $S_i^{-\bullet}$ in the absence of S_o and a bimolecular rate constant for an electron transfer from $S_i^{-\bullet}$ to S_o, respectively. Considering that the sensitizers are anchored at the bilayer–water interface by the carboxylate group, it is reasonable to think that the electron transfer across the vesicle bilayer proceeds not by a mechanism involving translocation of the sensitizer radical anion, but by an electron exchange mechanism. Finally, the efficiency Φ_A is depicted by $k_t[MV^{2+}]/(\tau_o^{-1} + k_t[MV^{2+}])$, which represents the efficiency for $S_o^{-\bullet}$ to transfer an electron to MV^{2+} in the outer aqueous phase, where τ_o is the lifetime of $S_o^{-\bullet}$ in the absence of MV^{2+}.

The dependence of the photogenerated $MV^{+\bullet}$ concentration on the irradiation time given by eqn (3) is fully consistent with the observed $MV^{+\bullet}$ accumulation curve, which was analyzed by first-order kinetics (eqn (1)). Thus, the observed initial rate of $MV^{+\bullet}$ formation, v_i, is found to be equal to $aI\Phi_D\Phi_E\Phi_A$, and the total quantum yield for $MV^{+\bullet}$ formation, Φ_t, defined in the previous section is identified as $a\Phi_D\Phi_E\Phi_A$.

(4) Dependence of the initial rate of $MV^{+\bullet}$ accumulation on MV^{2+} Concentration. In order to obtain evidence in support of the mechanism described above, the dependence of v_i on the initial concentration of MV^{2+} added to the outer aqueous phase, $[MV^{2+}]$, was examined. Assuming the above mechanism, v_i is depicted by $aI\Phi_D\Phi_E\Phi_A$. Since Φ_A is equal to $k_t[MV^{2+}]/(\tau_o^{-1} + k_t[MV^{2+}])$, a linear relationship between $1/v_i$ and $1/[MV^{2+}]$ is expected as shown in eqn (4).

$$1/v_i = (1/aI\Phi_D\Phi_E)(1 + 1/(k_t\tau_o[MV^{2+}])) \quad (4)$$

Fig. 3 shows plots of $1/v_i$ against $1/[MV^{2+}]$ for the electron transport across vesicle bilayers using **1a** and **1c** as sensitizers, which give straight lines as expected. As shown in the figure, the slopes of these two lines differ greatly, indicating that v_i for **1c** depends on $[MV^{2+}]$ more largely compared with **1a**. The least-squares analysis of the plots shown in Fig. 3 gives us the value of $k_t\tau_o$, which enables evaluation of the efficiency Φ_A. The Φ_A values for **1a** and **1c** are calculated to be 0.36 and 0.033 at $[MV^{2+}] = 10$ mM, respectively. This result suggests that the large decrease in v_i for **1c** compared with **1a** is mainly due to a considerably smaller value of Φ_A.

Table 3 Relative quantum yields for the electron transport across vesicle bilayers sensitized by **1a** and **1c**

Sensitizer	$v_i/10^{-7}$ M min^{-1}	I(rel)	Φ_t(rel)[a]	Φ_D	Φ_E(rel)[b]	Φ_A
1a	18.0	1.0	14.7	0.82	1.0	0.36
1c	2.5	3.9	0.51	0.94	0.33	0.033

[a] See Table 1. [b] Efficiency for $S_i^{-\bullet}$ to transfer an electron to S_o estimated by $\Phi_t(\text{rel})/(\Phi_D\Phi_A)$ ($\Phi_E(\text{rel}) = 1.0$ for **1a**).

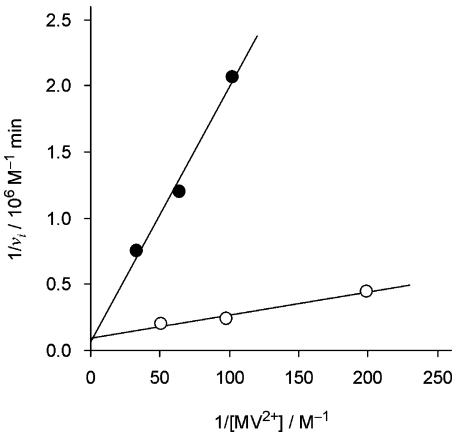

Fig. 3 Plots of a reciprocal of the initial rate of $MV^{+\bullet}$ formation *vs.* a reciprocal of the initial concentration of MV^{2+} for the irradiation of a solution of vesicles containing **1a** (○) or **1c** (●) and Asc^-.

The efficiencies estimated for individual processes of the electron transport across vesicle bilayers using **1a** and **1c** as sensitizers are presented in Table 3. Thus, it is concluded that the remarkable decrease in the total quantum yield of the electron transport, Φ_t, with an increase in the length of the methylene chain linking a carboxyl group with the pyrene nucleus is mainly attributed to a decrease in Φ_A, the efficiency for $S_o^{-\bullet}$ in the transfer of an electron to MV^{2+} in the outer aqueous phase, which is due to a decrease in the value of $k_t\tau_o$. Because the pyrene moiety of **1c** is located in the deeper interior of the vesicle membrane compared with that of **1a**, the rate constant for the electron transfer from $S_o^{-\bullet}$ to MV^{2+}, k_t, would be reduced owing to the longer distance of the pyrene moiety from the outer aqueous phase. Moreover, the back electron transfer from $S_o^{-\bullet}$ to S_i would be enhanced owing to the shorter distance between the pyrene moieties of S_i and S_o, which reduces the lifetime of $S_o^{-\bullet}$, τ_o. Thus, we propose that these two factors are responsible for the smaller value of Φ_t in the electron transport across vesicle bilayers using **1c** as a sensitizer compared with **1a**.

Design and syntheses of novel pyrene derivatives acting as excellent sensitizers

The initial rate of $MV^{+\bullet}$ formation, v_i, as well as the maximal concentration of photogenerated $MV^{+\bullet}$, C_{max}, is governed by two factors; the number of photons absorbed by the sensitizer in unit time, I, and the total quantum yield for $MV^{+\bullet}$ formation, Φ_t. As shown in Table 1, an increase in the hydrophobicity of a sensitizer causes an increase in its concentration in the vesicle solution, C_s, which is favorable for an increase in I, but decreases Φ_t because it is incorporated in the interior of the vesicle membrane. On the other hand, although the large Φ_t value is achieved in a hydrophilic sensitizer such as **1a**, which is located at the bilayer–water interface, it has limited solubility in the vesicle. Thus, in order to enhance v_i and C_{max} by using sensitizers with large values of both I and Φ_t, we designed novel unsymmetrically substituted bifunctional pyrenes **5a–c**. These pyrenes have both a carboxyl group linked with a short methylene chain, by which the pyrene moiety is placed at the bilayer–water interface facilitating an electron transfer from or to the species in the bulk aqueous phase, and a hydrophobic long alkyl group to increase solubility in the vesicle membrane.

Table 4 Electron transport across vesicle bilayers sensitized by bifunctional pyrenes **5a–c**

Sensitizer	$v_i/10^{-7}$ M min^{-1}	C_{max}/μM	C_s/μM	I(rel)[a]	Φ_t(rel)[b]
5a	43.5	29.3	53	13.2	2.6
5b	57.5	38.7	64	14.4	3.1
5c	46.2	29.0	74	15.3	2.3
1b	9.1	10.9	5.7	1.0	7.0

[a] Relative value of the number of photons absorbed by the sensitizer under irradiation estimated by the integration of $I_f(\lambda)(1–10^{-\varepsilon(\lambda)Csl})$ (I(rel) = 1.0 for **1b**). [b] Relative value of a total quantum yield for $MV^{+\bullet}$ formation (Φ_t = 10.0 for **2a**).[21]

The preparation route for these pyrenes is summarized in Scheme 2. Moreover, the result of the electron transport across vesicle bilayers obtained by using **5a–c** as sensitizers is shown in Table 4, together with that obtained by using **1b** under identical irradiation conditions.

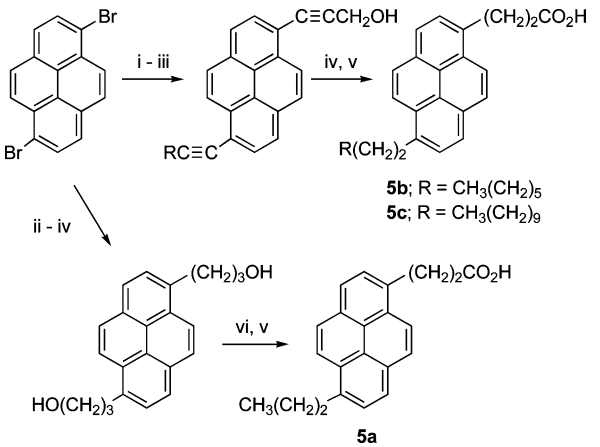

Scheme 2 Route for the preparation of unsymmetrically substituted bifunctional pyrenes **5a–c**. *Reagents and conditions*: i: H–C≡C–R, $Pd(Ph_3P)_2Cl_2$, CuI, morpholine; ii: H–C≡C–CH_2OTHP, $Pd(PPh_3)_2Cl_2$, CuI, morpholine; iii: pyridinium *p*-toluenesulfonate, EtOH–CH_2Cl_2; iv: H_2, PtO_2, THF; v: pyridinium dichromate, DMF; vi: MsCl, Et_3N, CH_2Cl_2 and then $LiBHEt_3$, THF.

As expected, the introduction of a hydrophobic alkyl group into the pyrene nucleus of **1b** causes a significant increase in v_i, as well as C_{max}. Although the relative value of I for each sensitizer is evaluated by the integration of $I_f(\lambda)(1 - 10^{-\varepsilon(\lambda)Csl})$ as shown in the previous section, it should be noted that the absorption maxima of **5a–c** are red-shifted by 7 nm compared with that of **1b** owing to the substitution of an alkyl group at the 6-position of the pyrene nucleus (Fig. 4). The values of I, as well as Φ_t which is evaluated by $\Phi_t = v_i/I$, for **5a–c** relative to those of **1b** are also presented in Table 4. As shown in the table, a significant increase in v_i observed

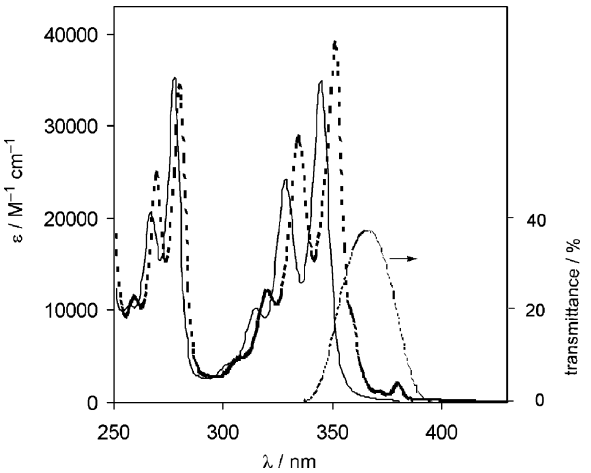

Fig. 4 UV–vis spectra of **1b** (solid line) and **5a** (broken line) in dichloromethane. The parabolic curve in the range of 360 ± 20 nm shows the wavelength dependence of the transmittance of the optical filter system employed in our experiments, $I_f(\lambda)$.

in the electron transport across vesicle bilayers by using **5a–c** as sensitizers is attributed to the large value of I which is due to their large solubility in the vesicle membrane increasing C_s, and the bathochromic shift of their absorption maxima increasing the absorptivity of the incident light. It should be pointed out that in spite of the high concentration of **5a–c** in the vesicle membrane,[26] only weak emission due to the excimer was observed at 480 nm (Fig. S7†), indicating that quenching of the excited sensitizer by the other pyrene is negligible.

Moreover, in spite of the substitution of a long alkyl chain, Φ_t's for **5a–c** are not so greatly reduced compared to that of **1b**, indicating the remarkable effect of a carboxylate group anchoring the pyrene moiety at the bilayer–water interface. The effect of the length of a hydrophobic alkyl chain on the electron transport efficiency was not observed, suggesting that a propyl group is sufficiently long to give **1b** sufficient solubility to vesicle membranes.

Conclusions

We found that an endoergic electron transport across vesicle bilayers from Asc^- in the inner waterpool to MV^{2+} in the outer aqueous solution can be driven by irradiation of pyrene derivatives embedded in the vesicle bilayers. The ability of the pyrene derivative as a sensitizer for the electron transport is dependent on the substituent group of the pyrenyl ring; a hydrophilic functional group linked with the pyrene moiety by a short methylene chain is necessary to act as an excellent sensitizer. We propose that electron transport is mainly initiated by the reductive quenching of the singlet excited state of the pyrene by Asc^- to produce the pyrene radical anion in the vesicle bilayer close to the inner waterpool, and proceeds by a mechanism involving electron exchange between the pyrenes located at the inner and outer interfaces across the vesicle bilayer. To validate this mechanism, however, the detection of reactive intermediates involving the electron transport across vesicle bilayers and the detailed analyses of their kinetic behaviors using time-resolved laser flash photolysis are required.[27] Moreover, we synthesized novel unsymmetrically substituted pyrenes having both a hydrophilic group linked by a short methylene chain and a hydrophobic long alkyl group, which act as excellent sensitizers for the electron transport across vesicle bilayers. Although this system unfortunately cannot work using visible light, it appears to be one of the most faithful models of natural photosynthesis in that an electron is transferred with the aid of light energy between two reversible redox couples in the energetically uphill direction through lipid bilayer walls preventing a charge recombination. Work is in progress to enhance the efficiency of the electron transport and to link this system with catalytic reactions to achieve the fixation of light energy into the chemical bond energy.

Experimental

General methods

^{1}H NMR spectra were recorded on a 270 or 500 MHz spectrometer. ^{13}C NMR spectra were recorded on a 125 MHz spectrometer. EI-MS spectra (70 eV) were obtained on a JMS-600H spectrometer. UV–vis spectra were recorded on a JASCO V-560 spectrometer. Fluorescence spectra were recorded on a JASCO FP-777 spectrofluorometer with a 200 nm min^{-1} scanning speed and a 1.5 nm bandwidth on excitation at 350 nm. Preparative thin-layer chromatography (PTLC) was carried out with Merck Silica Gel 60 F_{254}, and column chromatography was done with Cica-Merck Silica Gel 60. (1-Pyrenyl)acetic acid (**1a**), 4-(1-pyrenyl)butyric acid (**1c**), and (1-pyrenyl)methanol (**3a**) were purchased from Aldrich and used after recrystallization. (1-Pyrenyl)methylamine (**2a**) was obtained by treatment of its commercially available hydrochloride (Aldrich) with an alkaline solution. Phosphatidylcholine from egg yolks (PC) was purchased from Sigma-Aldrich, and *N*,*N*′-dimethyl-4,4′-bipyridinium dichloride trihydrate ($MVCl_2 \cdot 3H_2O$), sodium ascorbate (AscNa), and tris(hydroxymethyl)aminomethane (Tris) were purchased from Tokyo Kasei Kogyo Co., Ltd. and used without purification.

Vesicle preparation

A CH_2Cl_2 solution (1.77 mL) containing the sensitizer (0.52 mmol) and PC (12.0 mmol) was evaporated under reduced pressure to dryness in a test tube, coating the glass surface with a film of the amphiphile containing the sensitizer. To the test tube was added a solution (4 mL) of 1.0 M Tris–HCl buffer, pH 7.5, containing 1.0 M AscNa, and the amphiphile was dispersed by sonication for 60 min at 45 °C. During sonication Ar was bubbled into the solution. The resulting suspension was developed on a column with Sephadex G-50 (Amersham Biosciences) equilibrated with a 1.0 M Tris–HCl buffer solution containing 1.0 M NaCl, and the fraction (3.5 mL) containing the amphiphile was collected. To the solution (3.0 mL) was added $MVCl_2 \cdot H_2O$ (30 mmol) to give a vesicle solution for electron transport experiments. The concentration of the sensitizer in the vesicle solution, C_s, was evaluated by the absorbance at the wavelength of its maximal absorption and its molar extinction coefficient determined in a fluid solution; 345 nm ($\varepsilon = 35\,000$ M^{-1} cm^{-1}) for **1–4** and 352 nm ($\varepsilon = 39\,000$ M^{-1} cm^{-1}) for **5**.

Dynamic light scattering (DLS) studies

Vesicle solutions were prepared as described above. DLS measurements were made on a Honeywell Microtac UPA-150 at room temperature. The mean refractive index of 1.81 was used as the refractive index of the sample. The mean diameters of particles were calculated from volume distribution data obtained as the average of five measurements.

Photochemistry

A vesicle solution was placed into a quartz cell (10 mm × 10 mm), and Ar was bubbled into the solution for 60 min. The solution was irradiated with a 500 W xenon arc lamp through both a Toshiba optical cutoff filter (UV-35, >350 nm) and a band pass filter (UV-D36B, 360 ± 20 nm). The $MV^{+\bullet}$ accumulation was monitored by an increase in the absorption at 604 nm, and the concentration of $MV^{+\bullet}$, $[MV^{+\bullet}]$, was calculated by using its molar extinction coefficient ($\varepsilon = 12\,400\ M^{-1}\ cm^{-1}$).[4,28] In the electron transport in the presence of surfactant, 27 μM of Triton X-100 (Tokyo Kasei Kogyo Co., Ltd.) was added to the vesicle solution (3 mL) before irradiation. The concentration of Asc^-, $[Asc^-]$, was determined as follows: the irradiated vesicle solution was aerated to oxidize $MV^{+\bullet}$, and an aqueous solution of Triton X-100 (10% (w/w), 100 μL) was added to the solution. After stirring for 5 min, a $K_3[Fe(CN)_6]$ solution (30 mM) in 1.0 M Tris–HCl buffer containing 1.0 M NaCl was added, and $[Asc^-]$ was calculated on the basis of the consumption of $[Fe(CN)_6]^{3-}$ determined by a decrease in the absorption of 420 nm ($\varepsilon = 1027\ M^{-1}\ cm^{-1}$). In the experiment for dependence of the initial rate of $MV^{+\bullet}$ formation on light intensity, the vesicle solution was divided into four portions (3 mL each), and each solution was irradiated with 366 nm light emitted by an extra-high pressure mercury lamp (Ushio, SX-UI D500HAMP) through both an optical cutoff filter (UV-35, >350 nm) and a band-path filter (UV-D36B, 360 ± 20 nm). The light intensity was regulated by using four Toshiba neutral density filters, the transmittances of which for 366 nm light are 23.0, 12.5, 6.6, and 3.8%.

Fluorescence quenching studies

A vesicle solution for fluorescence quenching studies was prepared in the same manner as that described above, except for using 1.0 M NaCl instead of AscNa. Solutions of the sensitizer containing various amounts of quenchers were placed in quartz cells (10 mm × 10 mm). Fluorescence spectra were measured at room temperature under air on excitation at 350 nm. Relative fluorescence intensities (F_0/F) were determined by measuring the peak of heights for the maxima. The fluorescence lifetime was measured by using a pulsed Q-switch Nd:YAG laser (SOLAR LF114) as the excitation source. The fluorescence decay profiles were recorded by the use of third harmonic generation of the laser that provided UV pulses at 355 nm with a duration of 13 ns. A sample solution was placed in a quartz cell (10 mm × 10 mm), and the fluorescence was collected at 90° to the excitation light.

References

1 (*a*) J. Whitmarsh and Govindjee, in *Concepts in Photobiology*, ed. G. S. Singhal, G. Renger, S. K. Sopory, K.-D. Irrgang and Govindjee, Kluwer Academic Publishers, Dordrecht, 1999, p. 11; (*b*) B. Ke, *Photosynthesis*, Kluwer Academic Publishers, Dordrecht, 2001.

2 (*a*) M. Calvin, *Acc. Chem. Res.*, 1978, **11**, 369; (*b*) M. Calvin, *Energy Res.*, 1979, **3**, 73; (*c*) T. Meyer, *Acc. Chem. Res.*, 1989, **22**, 163; (*d*) D. Gust, T. A. Moore and A. L. Moore, *Acc. Chem. Res.*, 2001, **34**, 40; (*e*) D. Gust, T. A. Moore and A. L. Moore, in *Aritificial Photosynthesis*, ed. A. F. Collings and C. Critchley, Wiley, Weinheim, 2005, p. 187.

3 (*a*) A. D. Bangham, *Prog. Biophys. Mol. Biol.*, 1968, **18**, 29; (*b*) D. W. Deamer and P. S. Uster, in *Liposomes*, ed. M. J. Ostro, Marcel Dekker, New York, 1983, p. 27.

4 W. E. Ford, J. W. Otvos and M. Calvin, *Nature*, 1978, **274**, 507.

5 For reviews of electron transfer across membranes, see: (*a*) J. N. Robinson and D. Cole-Hamilton, *Chem. Soc. Rev.*, 1991, **20**, 49; (*b*) S. V. Lymar, V. N. Parmon and K. I. Zamaraev, *Top. Curr. Chem.*, 1991, **159**, 1.

6 L. Zhu, R. F. Khairutdinov, J. L. Cape and J. K. Hurst, *J. Am. Chem. Soc.*, 2006, **108**, 825.

7 T. Katagi, T. Yamamura, T. Saito and Y. Sasaki, *Chem. Lett.*, 1981, 1451.

8 A. A. Krasnovsky, A. N. Semenova and V. V. Nikandrov, *Photobiochem. Photobiophys.*, 1982, **4**, 227.

9 (*a*) S. Murata, R. Nakatsuji and H. Tomioka, *J. Chem. Soc., Perkin Trans. 2*, 1995, 793; (*b*) S. Ikeda, S. Murata, K. Ishii and H. Hamaguchi, *Bull. Chem. Soc. Jpn.*, 2000, **73**, 2783.

10 For a preliminary report, see: A. Yoshida, A. Harada, T. Mizushima and S. Murata, *Chem. Lett.*, 2003, **32**, 68.

11 For the calclulation of the free-energy change for the total redox reaction, +0.09 V and −0.46 V were employed for the redox potentials of $Asc^{\bullet}/Asc^-$ (pH 7.0)[12a] and $MV^{2+}/MV^{+\bullet}$[12b] (*vs.* SCE), respectively.

12 (*a*) D. Njus and P. M. Kelly, *Biochim. Biophys. Acta*, 1993, **1144**, 235; (*b*) S. L. Murov, I. Carmichael and G. L. Hug, *Handbook of Photochemistry*, 2nd edn, Marcel Dekker, New York, 1993.

13 (*a*) M. Aikawa, N. J. Turro and K. Ishiguro, *Chem. Phys. Lett.*, 1994, **222**, 197; (*b*) L. Li and L. K. Patterson, *Photochem. Photobiol.*, 1995, **62**, 51.

14 (*a*) Y. Barenholz, T. Cohen, R. Korenstein and M. Ottolenghi, *Biophys. J.*, 1991, **59**, 110; (*b*) Y. Barenholz, T. Cohen, E. Haas and M. Ottolenghi, *J. Biol. Chem.*, 1996, **271**, 3085; (*c*) S. J. Webb, K. Greenaway, M. Bayati and L. Trembleau, *Org. Biomol. Chem.*, 2006, **4**, 2399.

15 (*a*) H. Schomburg, H. Staerk and A. Weller, *Chem. Phys. Lett.*, 1973, **22**, 1; (*b*) Y. Hirata, T. Saito and N. Mataga, *J. Phys. Chem.*, 1987, **91**, 3119; (*c*) X. Liu, K.-K. Iu and J. K. Thomas, *Chem. Phys. Lett.*, 1993, **204**, 163.

16 The irradiation of the vesicle solution with the shorter wavelength light causes direct excitation of MV^{2+} having an intense transition with a maximum at 259 nm ($\log \varepsilon = 4.2$ in Tris–HCl buffer, pH 7.5) and weak tailing to *ca.* 350 nm, which leads to the $MV^{+\bullet}$ formation even in the absence of the sensitizer.

17 It was reported that a long-lived reduced MV^{2+} derivative was produced by the irradiation of a lipid functionalized pyrene in vesicles even in the absence of an electron donor, which is probably due to the scavenging of the pyrene radical cation by the double bond of lipid molecules.[13].

18 In the case of the irradiation using (1-pyrenyl)methylamine (**2a**) as a sensitizer, *ca.* 30% of $MV^{+\bullet}$ was accumulated even in the absence of Asc^-, which is probably due to an irreversible electron donation of the amino group of **2a** (Fig. S3†).

19 (*a*) D. C. Dong and M. A. Winnik, *Photochem. Photobiol.*, 1982, **35**, 17; (*b*) D. C. Dong and M. A. Winnik, *Can. J. Chem.*, 1984, **62**, 2560.

20 J. Luisetti, H. Möhwald and H.-J. Galla, *Biochim. Biophys. Acta*, 1979, **552**, 519.

21 The quantum yield for $MV^{+\bullet}$ formation sensitized by (1-pyrenyl)methylamine (**2a**) in the vesicle solution was determined to be 0.10 using a photon counting meter (Ushio, UIT-150) under irradiation with 366 nm light of a 500 W extra-high-pressure mercury lamp (Ushio, SX-UI D500HAMP).[10] Thus, in the tables, the relative quantum yields for $MV^{+\bullet}$ formation, Φ_t(rel), are represented using **2a** as a standard.

22 S. C. Wallace, M. Grätzel and J. K. Thomas, *Chem. Phys. Lett.*, 1973, **23**, 359.

23 D. Rehm and A. Weller, *Isr. J. Chem.*, 1970, **8**, 259.

24 For the calculation of the free-energy change for the photoinduced electron transfer, +1.16 V, −2.09 V, and 76.7 kcal mol^{-1} were employed

for the oxidation potential of pyrene (E_{ox} *vs.* SCE), the reduction potential of pyrene (E_{red} *vs.* SCE), and the excited singlet energy of pyrene (E_s), respectively[12b].
25 W. E. Ford, J. W. Otvos and M. Calvin, *Proc. Natl. Acad. Sci. U. S. A.*, 1979, **76**, 3590.
26 Since the concentration of PC molecules in the solution used in our electron transport experiments is *ca.* 6 mM, a molar fraction of the sensitizer incorporated in the vesicle solution at $C_s = 60$ μM is approximately 1%.
27 We preliminarily performed laser flash photolysis studies for the detection of reactive species involving the electron transport across vesicle bilayers sensitized by (1-pyrenyl)acetic acid (**1a**) by using a pulsed Q-switch Nd:YAG Laser (SOLAR LF114) as the excitation source (355 nm, 20 ns, 4 mJ pulse^{-1}). We could observe both a radical cation (445 nm) and a radical anion (493 nm) of **1a**, as well as the triplet excited state of **1a** (428 nm), having a lifetime of 2–5 μs. However, these radical ions could be detected by the irradiation of vesicle solutions containing **1a** even in the absence of Asc^- and MV^{2+} due to the photoinduced charge separation between the pyrenes embedded in the vesicle membrane. Thus, in order to identify the reactive species involving the electron transport, detailed analysis of the dynamic behaviors of these reactive species using more sophisticated apparatus is required.
28 E. Steckhan and T. Kuwana, *Ber. Bunsen-Ges.*, 1974, **78**, 253.

